SEMI-ANNUAL PROGRESS REPORT
NAG8-708-1

HIGH TEMPERATURE FURNACE MODELING AND PERFORMANCE VERIFICATIONS

Submitted to

Richard M. Poorman
Mail Code JA62
George C. Marshall Space Flight Center
National Aeronautics and Space Administration
Huntvsille, Alabama 35812

Prepared by

James E. Smith, Jr., Ph.D.
Associate Professor and Director
Chemical Engineering Program

Department of Mechanical Engineering
College of Engineering
The University of Alabama in Huntsville
Huntsville, Alabama 35899

October 1988

Table of Contents

SEMIANNUAL PROGRESS REPORT
HIGH TEMPERATURE FURNACE MODELING
AND PERFORMANCE VERIFICATIONS

1.0 INTRODUCTION

Under NASA Grant NAG8-708 we are performing analytical, numerical, and experimental studies on two classes of high temperature materials processing furnaces. The research concentrates on a commercially available high temperature furnace using zirconia as the heating element and an Arc Furnace under design at NASA's MSFC, based on a ST International tube welder. The zirconia furnace has been delivered and the work is progressing as scheduled. The work on the Arc Furnace was initially stalled due to the unavailability of the NASA prototype, which is actively being tested aboard the KC-135 experimental aircraft. A proposal was written and funded to purchase an additional arc welder to alleviate this problem. The ST International weld head and power supply have been received and testing will begin in early November. The following progress report covers the first 6 months of this grant.

1.1 OBJECTIVES

There were four major objectives during this reporting period. The first objective was to assemble the zirconia furnace and construct components needed to successfully perform a series of experiments. The second objective was to evaluate the furnace's performance as-delivered from the manufacturer and investigate methods of improving its performance. A high temperature optical pyrometer was purchased and integrated with the furnace using a specially manufactured mount. The third objective was establish a data base on materials used in furnace construction, with particular emphasis on emissivities, transmissivities and absorptivities as functions of wavelength and temperature. These data are being used to develop a one-dimensional spectral radiation heat transfer model for comparison with standard effective radiation heat transfer modeling techniques. Modeling will eventually be used to predict wall and crucible temperatures needed to effectively apply open loop control techniques to advanced high temperature resistance and arc furnaces. Finally, a SINDA model developed for the MSFC Arc Furnace was

used to begin preliminary numerical designs of sample holders and to estimate cooling media temperatures for the steady-state operation of the furnace.

Objective 1. One of the focuses of this research project is the evaluation and performance verification of existing furnace technologies. Two furnace types are being considered. They are the ARTCOR Model 460-15 Bench Top Tubular Laboratory Research Furnace and an Arc Furnace being constructed at NASA's MSFC which uses a ST International Orbital Tube Welding System as a heat source. This report's first three sections concentrate on the ARTCOR Research Furnace. The first section discusses the initial assembly and evaluation of the manufacturer's instruction manual.

Objective 2. The second section contains an initial performance analysis of the zirconia furnace. The performance of the zirconia furnace was tested at different levels of applied power to the main zirconia heating element, namely 15%, 20%, 25% and 30%. The axial temperature profiles in the furnace were measured along the centerline for applied powers of 20% and 30%. Step change increase from 20% to 30% applied power and a linear ramp rate of 1% per minute from 0% to 15% applied power were studied.

Objective 3. Experimental data on various ceramics and other materials needed for eventual design construction and modeling of advance high temperature electrical furnaces were collected from various literature references. Spectral radiation data were collected on alumina, zirconia, and titania. These data were assembled to evaluate the material's emissivity, transmissivity, and absorptivity trends at various wavelengths and applied temperatures. Data for zirconia were used to estimate the effective emissivity for use with the high temperature optical pyrometer. Finally, the thermal and frequency characteristics of these data were used to formulate a one dimensional spectral model for comparison with effective radiation modeling approaches. A FORTRAN Computer program is being developed to solve this one-dimensional nonlinear problem. These efforts are being coordinated with those of the UAH Center for Microgravity Studies to prevent duplication and to accelerate development of advanced high temperature material processing technologies.

Objective 4. Numerical Analysis of the MSFC Arc Furnace. An Arc Furnace for use on the KC-135 experimental aircraft was first proposed by Poorman (1986). The furnace uses an ST International rotating tubular welding head and power supply to produce localized and extremely high temperatures. Several preliminary tests were conducted by Poorman on samples of Al, Cu and W using the configuration shown in Figure 1. We are in the process of numerically characterizing the processes and design parameters involved in the development of the Arc Furnace for use as a directional solidification furnace at temperatures exceeding those currently available, i.e. 1600°C. This portion of the research is directed towards developing scenarios for sample support, external furnace shielding, translation mechanisms, temperature limitations, and extensions of numerical characterizations to nonmetallic materials. Ultimately, the influences of electric fields on the microstructure of ferro, para, and nonmagnetic materials will have to be experimentally evaluated.

A numerical model developed for the Arc Furnace is described in the following sections and was applied to a sample holder with physical properties of stainless steel. The goal of this numerical study was to estimate the performance of stainless steel holders under various isothermal external boundaries. The external boundary was held constant at temperatures consistent with air, water, and oil cooling (10, 38, 50, 100, 150 and 200°C). Axial and radial profiles were determined for 75 mm long samples of tungsten held at each end by 25 mm long stainless steel holders.

2.0 RESULTS AND DISCUSSION

2.1 OBJECTIVE 1.

The ARTCOR zirconia furnace was received from NASA and required substantial assembly. A stand was required to support the furnace, optical pyrometer, and ventilator. This stand was designed to protect the furnace from vibrations and was fitted with clamps to hold accessories needed during the experiments. The stand, optical mount, and ventilator assembly were constructed at the UAH.

2.1.1 Assembly of the ARTCOR furnace.

Several problems were found during the assembly of this furnace which will

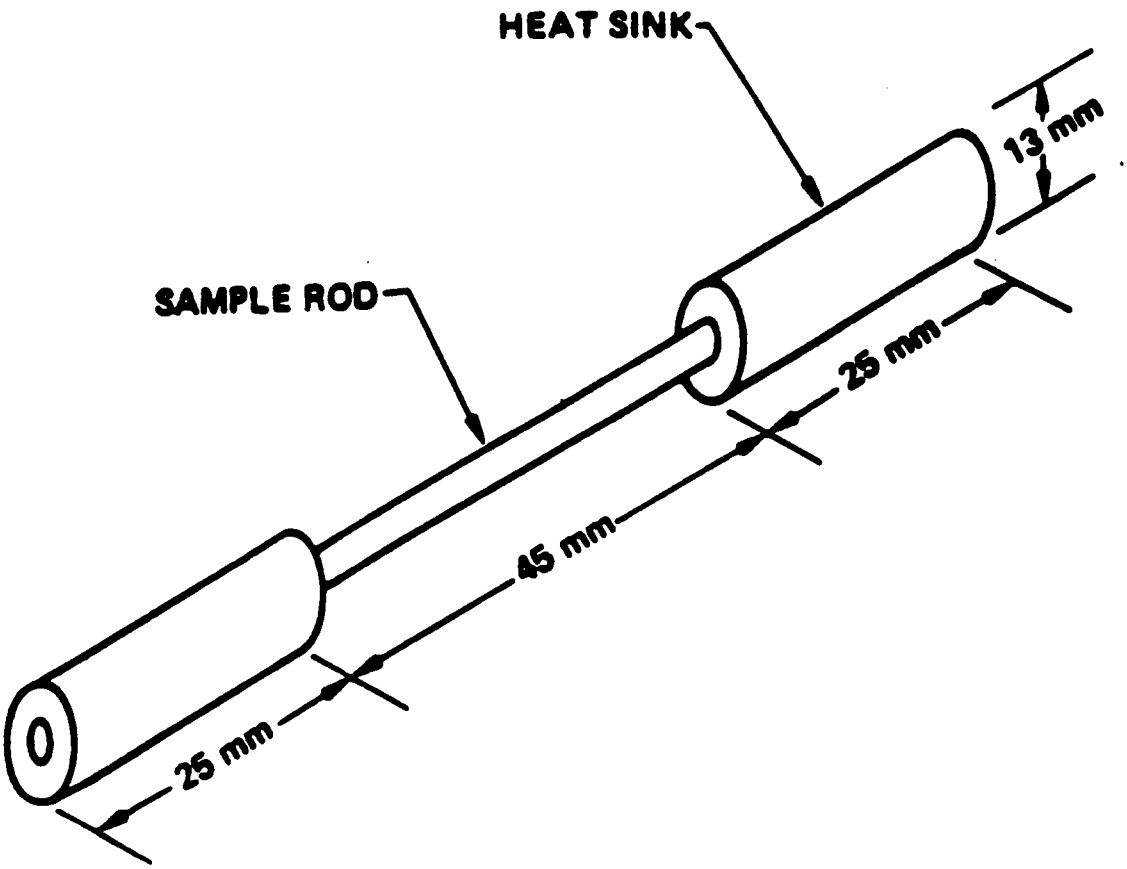

Figure 1. Arc Furnace sample and holder configuration as used by Poorman (1986).

be briefly discussed. In some cases, minor modifications of the instruction manual are suggested. The first problem encountered concerned the insertion of the furnace preheater module. When inserting the preheater module (Manufacturer's Manual Figure 12), it was realized that the diameter of the preheater module would not fit into the housing. The module was filed and sanded until it fully seated in the housing. In all, several adjustments had to be made before the module would properly fit the housing. Further, it was noted that the preheater module could not be installed because three wires tagged MAIN HEATER, HEATER and PREHEATER protruded into the housing. These wires had to be pushed back into their lead tube, the module inserted and later the wires pulled out to make proper connections to the furnace elements.

During the first two trial runs it was realized that the main heater element would not conduct because it was not reaching proper operating temperatures. The manufacturer was consulted and suggested that the preheat time be increased from 36 minutes to 48 minutes. The change was made but did not improve the situation, and after a second consultation, the manufacturer suggested an increase in the power input to the preheater from 40% to 43%. After this adjustment the main heater became operative and a successful run was made. A major problem with this furnace resides in its control program which controls the percentage of applied power to the preheater and zirconia element rather than controlling the process temperature. Thus the controller has no feedback or direct control of the process temperature.

A second trial run was made, however on this run the controller did not supply power to the heating elements. After analyzing the operating mode of the furnace controller and after contacting the controller manufacturer, it was determined that the controller did not self initialize after a given run. It is absolutely necessary that the operating instructions on page 17 of the manual include the procedure for reinitializing the controller as follows;

> To initialize the controller the two buttons on the front panel that are used to increase/decrease the process variables should be depressed simultaneously for a few seconds.

During the study it was found that the control module had to be manually

initialized at the start of every run. The controller is preprogrammed to perform specific functions by the supplier. In the early stages, the controller turns the preheater on at 20% applied power. It later ramps the applied power to 40% at a rate of 1% per minute. The preheater is then held at 40% power for a specified time to allow the main heating element to reach its conducting temperature. The supplied settings for this controller were not sufficient to reach the zirconia element conduction temperature. Further, since the controller has no positive feedback from the furnace, the fact that the zirconia element does not reach conduction temperature goes unnoticed. We have routinely adjusted both the soak time of the preheater and the power applied to the preheater to achieve conduction of the zirconia element. After several runs, it was found that the main-heater element would conduct only when the furnace had reached a temperature of at least 530°C. This temperature is important as above 530°C the zirconia element becomes a conductor, while below this temperature it responds as an insulator. Once the program has been modified to achieve zirconia conduction, the performance of the furnace in the future is not necessarily guaranteed. As an example, parameters which would start the zirconia element during one test would not restart the element after sitting cold for several days. At this point in the characterization and performance verification a fundamental problem with this system has been determined, namely, one of control. In discussions with the controller manufacturer we learned that the controller may be easily modified to communicate with a computer. Further, the optical pyrometer ordered for the system also has the ability to communicate with a computer. Modifications such as these could overcome many of the control problems outlined above.

After modifying the furnace assembly procedures and determining controller settings for proper furnace operations we began an experimental analysis of the furnace's performance.

2.2 OBJECTIVE 2.

2.2.1 Performance Verifications.

In the following section one requirement was that the furnace initially be evaluated in an as-received condition. No efforts were made to improve, modify, or alter in any way its geometry, heat transfer characteristics, or control routines. It should be noted that free convection is used to cool the

furnace casing. Also, since the furnace ends are open to the atmosphere, one recognizes that free convection and radiation losses will play major roles in the furnace's performance. Attempts to utilize this furnace for materials processing will require correction of these limitations.

In the following section we discuss preliminary performance verifications and attempts to characterize controller behavior. The controller was programmed to power the main heater at element at 15% to 30% applied power and the temperature responses of the heater studied. The goals was to partially calibrate the furnace temperature as a function of applied power. The temperatures measured for different applied power outputs to the main-heater element are given in Table 1.

Table 1.
Temperature of Furnace at Selected Applied Power*

APPLIED POWER (% of Maximum Power)	TEMPERATURE (°C)
15	834
20	950
25	1039
30	1145

* Temperatures measured at 1 inch from furnace bottom using a type K thermocouple.

Figure 2a shows temperatures measured by a thermocouple immersed along the centerline of the furnace as a function of applied power. Least squares regression of the data produced the linear relationship shown. The slope of the resulting function indicates that an approximate ratio of the increases between % applied power and furnace temperature approaches 1:20. Of course, a minimum applied power is required to achieve the zirconia conduction.

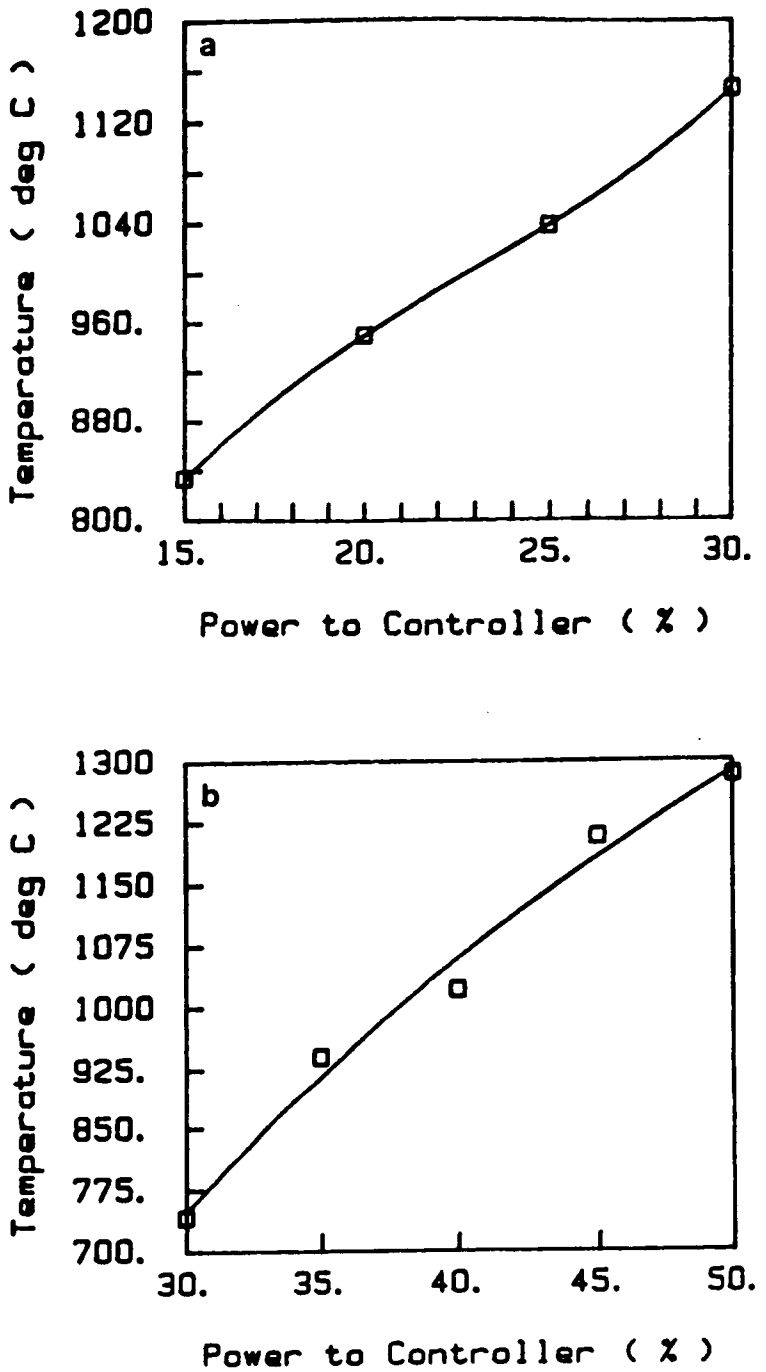

Figure 2. Temperature as a function of applied power for the ARTCOR Model 460-15 Furnace as measured by; a) a thermocouple immersed along the centerline of the furnace. b) a water-cooled optical pyrometer through the furnace wall viewing port provided by the manufacturer.

Work has also been completed on a special mount to accurately position a high temperature optical pyrometer to measure wall temperatures in the zirconia furnace. This mount provides very precise positioning of the pyrometer for consistent temperature measurements. In Table 2 are shown results obtained using the water-cooled optical pyrometer to measure the furnace temperature as recommended by the manufacturer. A small viewing port was provided by the manufacturer in the side of the furnace for direct viewing the zirconia heating element with the pyrometer. In Table 2, we attempted to match the temperatures measured by the thermocouple in Table 1 with that of the optical pyrometer, by manipulating the applied power to the furnace. A comparison of Tables 1 and 2 show that power levels almost twice as great were required to achieve similar temperature readings with the pyrometer as compared to the thermocouple.

Table 2.
Temperature of Furnace at Selected Applied Power*

APPLIED POWER (% of Maximum Power)	TEMPERATURE (°C)
30	742
35	951
40	1022
45	1208
50	1282

* Temperatures measured by optical pyrometer through furnace wall viewing port.

Figure 2b shows temperatures measured by the water-cooled optical pyrometer as a function applied power. It should be noted that the use of an optical pyrometer was recommended by the manufacturer as a method for calibrating furnace temperatures. In fact, an optical pyrometer was used by the manufacturer to calibrate the furnace prior to shipping. One questions the actual upper operating limit of this furnace when consideration is given to the

magnitude of the disparity presented in Tables 1 and 2. The manufacturer indicates that this furnace is capable of operating at 2000°C. Based on the above findings the upper limit operating temperature may be higher. In addition, temperature vs. applied power shows a slightly non-linear trend at higher temperatures as would be expected from radiation dependent devices, such as optical pyrometer. Thus any control algorithm that would employ an optical pyrometer should include non-linear terms.

To investigate the axial centerline temperature gradient, the furnace was held at applied powers of 20% and 30%. The temperature was allowed to stabilize before the readings were taken using a type K thermcouple positioned on the centerline line of the furnace tube (see Table 3). Figure 3 shows the measured axial temperature gradient for 20% applied power, while Figure 4 shows the results at 30% applied power. Axial gradients of approximately 250°C per inch were determined for both figures. Temperatures were found to be higher at the top of the furnace than at the equivalent distance from the furnace bottom as would be expected form a freely convecting media.

Table 3
Axial Temperature Variations Within the Furnace

DISTANCE FROM TOP (Inches)	TEMPERATURE (°C)
0.5	1106
0.8	1170
3.2	1147
3.5	900

* Temperatures measured at 1 inch from furnace bottom using a type K thermocouple.

Figure 5 shows the temperature response to a gradual increase in power at a linear rate of 1% per minute. The goal of this experiment was to investigate the furnace responds to a gradual increase in applied power. We were

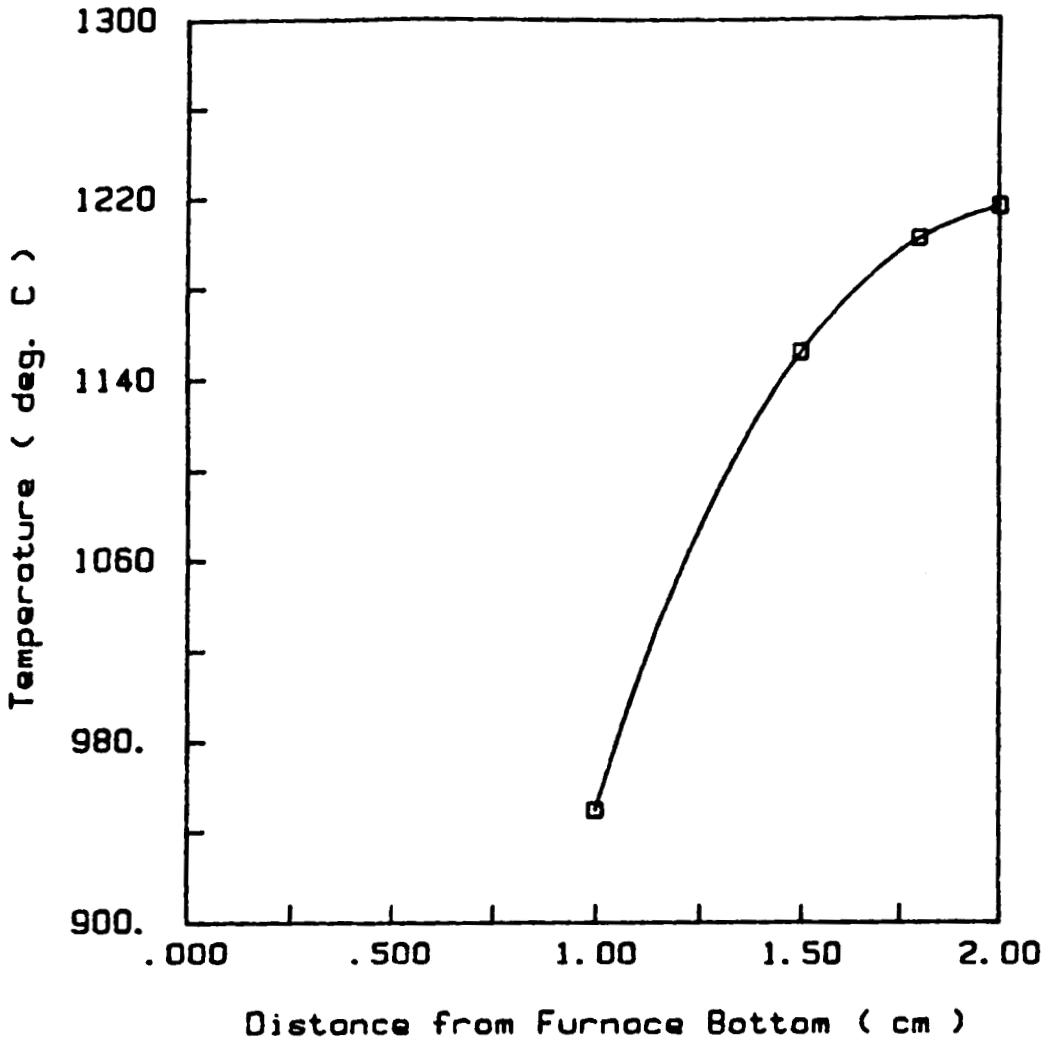

Figure 3. Axial temperature profile for the ARTCOR Model 460-15 Furnace at 20% applied power on the controller

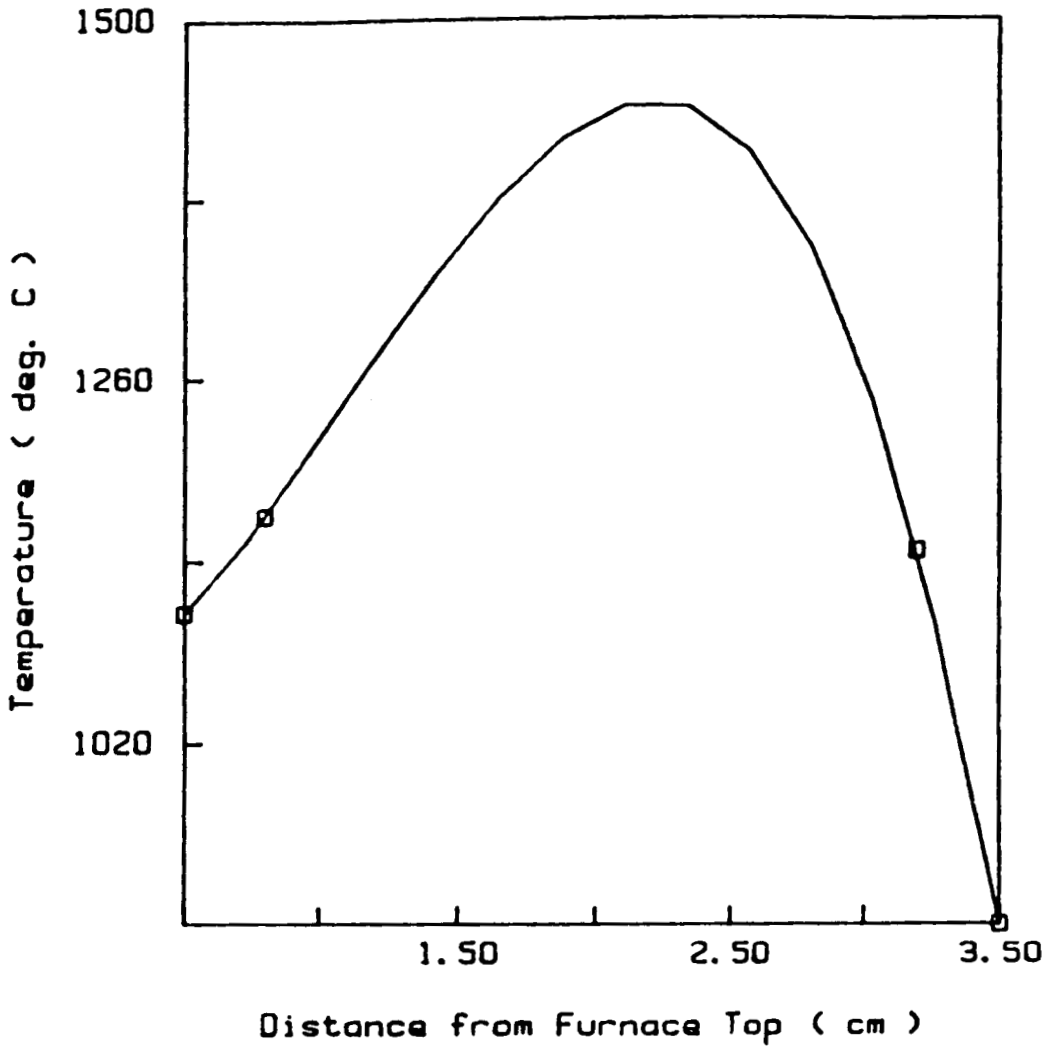

Figure 4. Temperature profiles for the ARTCOR Model 460-15 Furnace at 30% Power on the Controller.

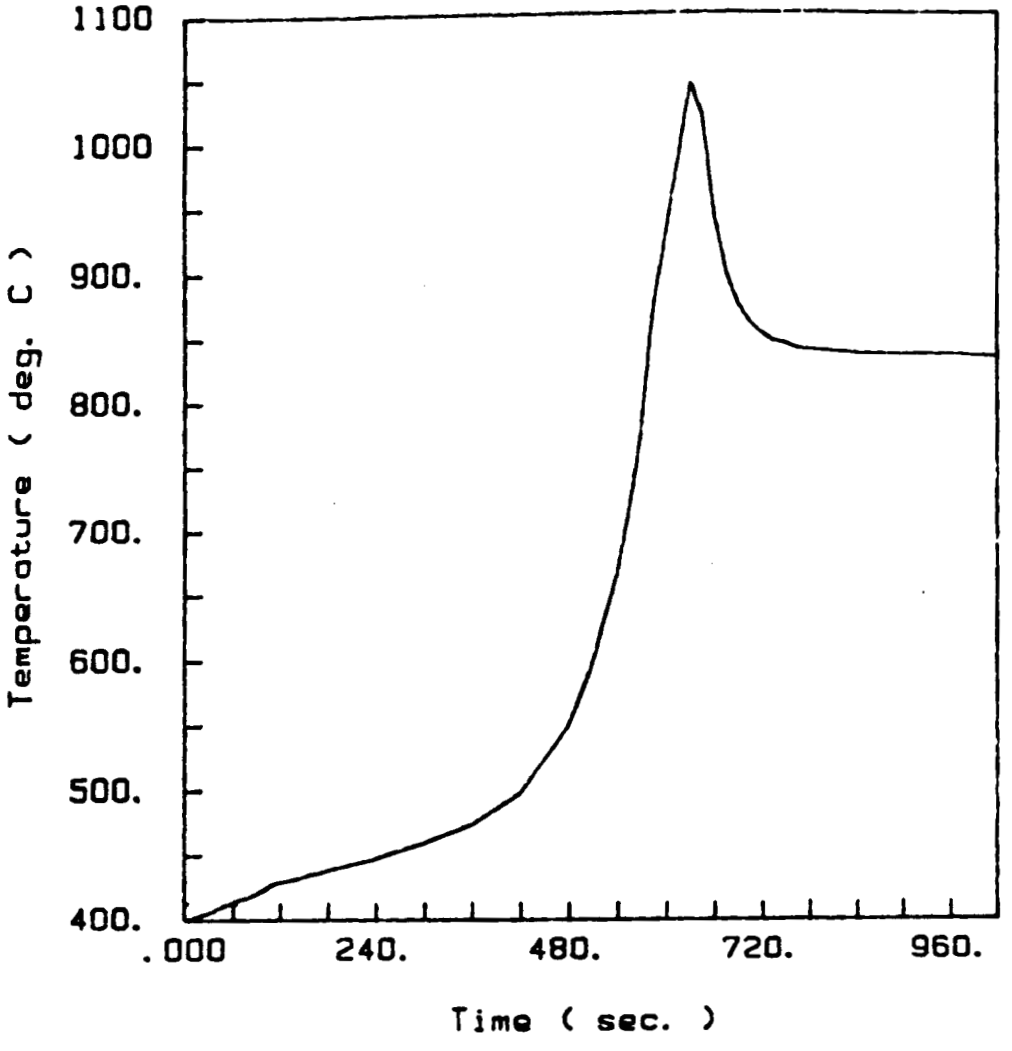

Figure 5. Temperature response for the ARTCOR Model 460-15 Furnace to a linear applied power increase at a rate of 1% per minute. Final applied power was 15%.

particularly intrested in set-point overshoot. The ratio of the increase in temperature to applied power was found to be approximately 15/1. A temperature overshoot of almost 200°C was recorded even at this gradual heating rate. Overshooting the process set-point is a persistent problem encountered when using the manufacturer's supplied controller.

During this series of tests, the controller developed a consistent error. The manufacturer was contacted and the device returned for repair. The repaired controller has been received and tested. Performance verifications of the zirconia furnace can now be continued.

2.3 OBJECTIVE 3.

In order to improve the performance of the furnace, an accurate model for the furnace has to be developed. A study is in progress to examine detailed heat transfer modeling through an alumina crucible which takes into account the various radiation heat transfer modes which are functions of temperature and wavelength. The detailed model is being developed for comparison with routine radiation heat transfer models which uses bulk radiation properties. A literature search was conducted on the spectral properties of furnace materials of construction, namely alumina, zirconia, and titania. In addition, thermal properties of iron were also found and will be used in the numerical analysis. Radiation properties, which are functions of wavelength, will be used to predict the radiation heat transfer of the crucible wall. At issue is the direct coupling of the sample to the furnace wall at specific frequencies for which the crucible wall is transparent. The model will also take into account the absorption and conduction of the crucible wall to the iron sample.

2.3.1 Numerical Analysis

We are actively developing a one-dimensional radiation-conduction problem where spectral properties like transmissivities, absorptivities, and emissivities will be considered as functions of wavelength and temperature. In this analysis the furnace wall will be considered as a black body emitting radiation at 1600°C through a vacuum to an alumina crucible containing an iron sample. The problem has been formulated into three distinct regions and two boundary conditions as shown in Figure 6. The furnace wall, set at a constant temperature of 1600°C, will serve as an isothermal boundary. Region 1 contains a vacuum, where radiation is the only mode for heat transfer. Region

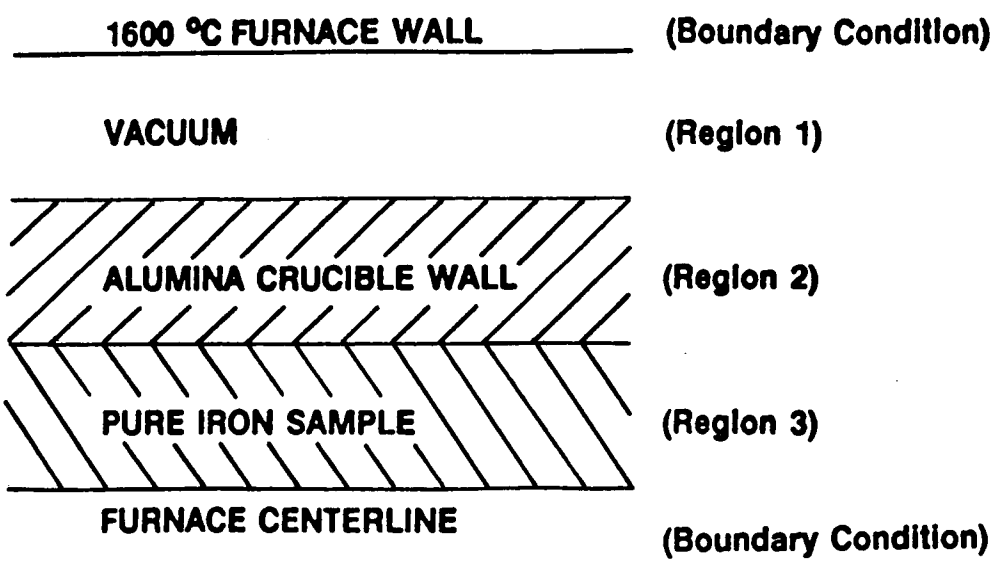

Figure 6. Detailed Radiation-Conduction Model which will take into account Spectral Radiation Properties of the Alumina Crucible Wall.

2 will be the crucible wall where both radiation and conduction play major roles in the transfer of heat. Heat transfer in region 3 (iron sample) is assumed to occur only by conduction. The numerical model is being developed to permit incorporation of other sample types, gaseous media, and/or furnace construction materials which may change the spectral properties of high temperature furnaces. Detailed heat transfer characteristics will play an important role in design and construction of the next generation of high temperature furnaces.

Progress on the radiation model has been slowed due to instabilities imposed by either the functions or the numerical technique chosen to solve this highly non-linear problem. Though the solutions obtained to date show the correct trends, the solution tends to oscillate as we increase the number of nodes in this finite-difference model. Polynomials were used to correlate emissivity, transmissivity, and absorptivity data as a function of wavelength and when these functions are integrated into the fourth order function which characterizes radiation heat transfer models, they may be combining to produce the instabilities we are observing. We are working to isolate and correct the source of this instability.

2.4 OBJECTIVE 4.

A numerical model of the Arc Furnace has been developed to evaluate a conceptual design based on the work of Poorman. The studies were made using an idealized model with the configuration shown in Figure 1, but with a sample rod only 20 mm long. Steady state idealized models of the Arc Furnace were numerically simulated using SINDA. This numerical model assumed symmetry; therefore, only half the configuration was modeled. Additionally, temperatures in the circumferential direction were assumed constant. The numerical model consisted of a 6.35mm O.D. x 70mm long sample of pure tungsten rod with 25mm of rod inserted into each holder of 13mm O.D. x 25mm long stainless steel. This configuration provides only a 20mm long tungsten sample rod. Since, symmetry was assumed, only 10mm of the sample rod and one heat sink required numerical modeling. We limited our numerical analysis to a sample length of 70mm, since this is our current experimental limit for preparing such a sample by powdered metal sintering techniques. Rods of pre-sintered materials of these dimensions can currently be prepared in our Craver press which has an applied force limited to 50,000

lbs/in^2 and a 300°C environmentally controlled pre-sintering furnace of original design. The numerical and experimental capabilities can easily be extended to a longer sample length.

The model developed included an isothermal boundary imposed at the end of the sample rod. The isothermal temperature was maintained at the melting point of pure tungsten (3387°C). The isothermal surface of the stainless steel holder was set at the temperatures consistent with air, water and oil cooling (10-200°C). Additionally, it was assumed that there was zero contact resistance between the tungsten sample rod and the stainless steel heat sink. An idealized radiation boundary was imposed on the exposed surface of the sample. This surface was radiation coupled to a constant 45°C environment and was a assumed to be a sufficient distance away from this environment to make the view factor F12 equal 1. The emissivity of tungsten at 3315.5°C, was assumed constant at 0.39 (Holman, 1981). To simplify the model, radiation exchange between the sample and sample holder was initially neglected.

The model was developed on a 1mm grid spacing which required 222 nodes, with additional nodes for radiation to the environment. The steady state solutions took approximately 3 minutes of computer core time. The actual performance of the experimental furnace, processing a tungsten sample, should fall below this idealized cases, due to the steady state assumption.

The power consumption as a function of the temperature of the quench block is shown in Figure 7. Power consumption ranges from 1.76 to 1.70 KW at a quench block temperature of 10 and 200°C, respectively. An increase in power of 0.32 watts is required for each degree centrigrade when the quench block temperature is operated below 200°C. Values discussed here and in the figure are within the experimentally range determined by Poorman (1986) for his 3.2mm diameter tungsten sample. Centerline axial temperature profiles for tungsten samples calculated at various quench block temperatures are shown in Figure 8. An axial centerline gradient of 2650°C was calculated for the first 3mm of the sample. Figure 8 shows that this gradient is virtually constant for the first 2-3mm on either side of the arc's location for the quench block temperatures imposed. The holder's isothermal boundary begins to influence the axial gradient in the sample at a distance of about 5mm from the arc's

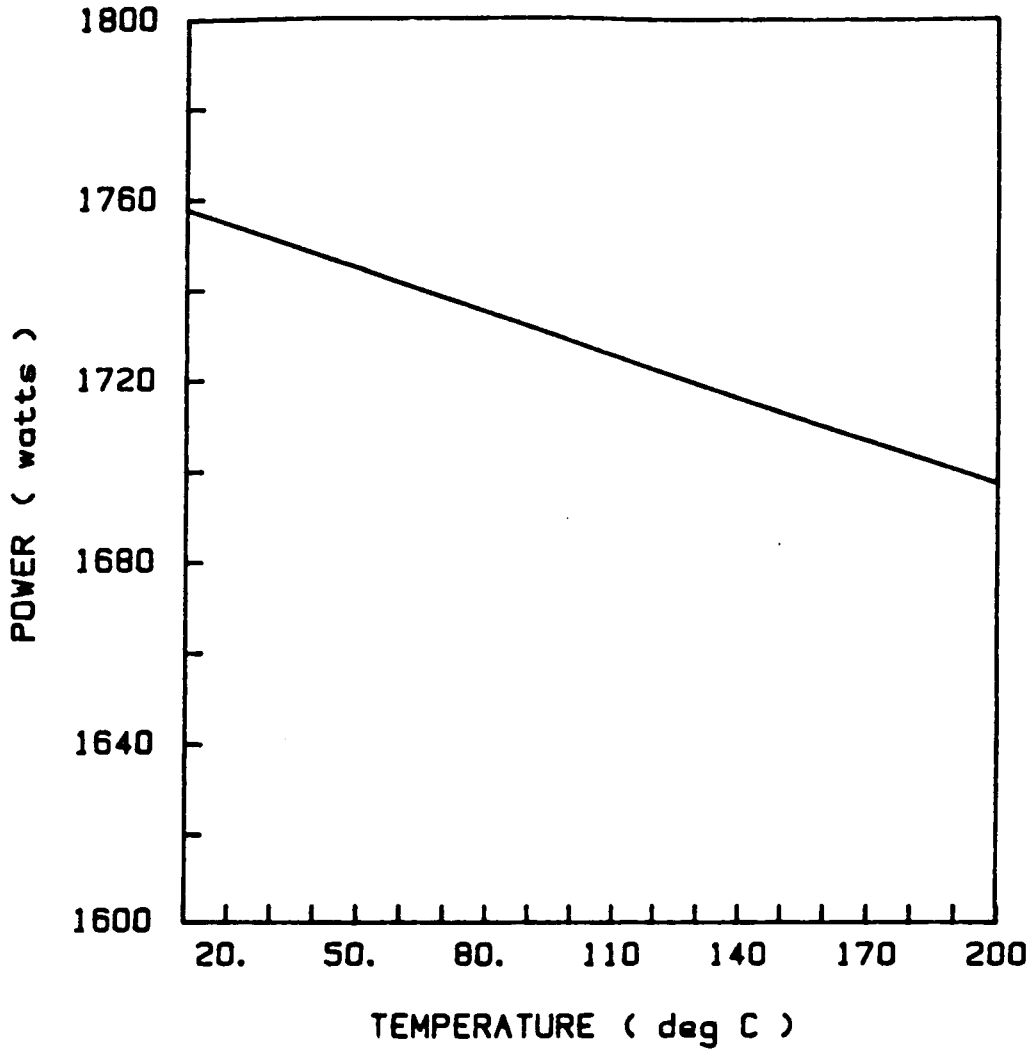

Figure 7. Steady-state power required for different quench block temperatures.

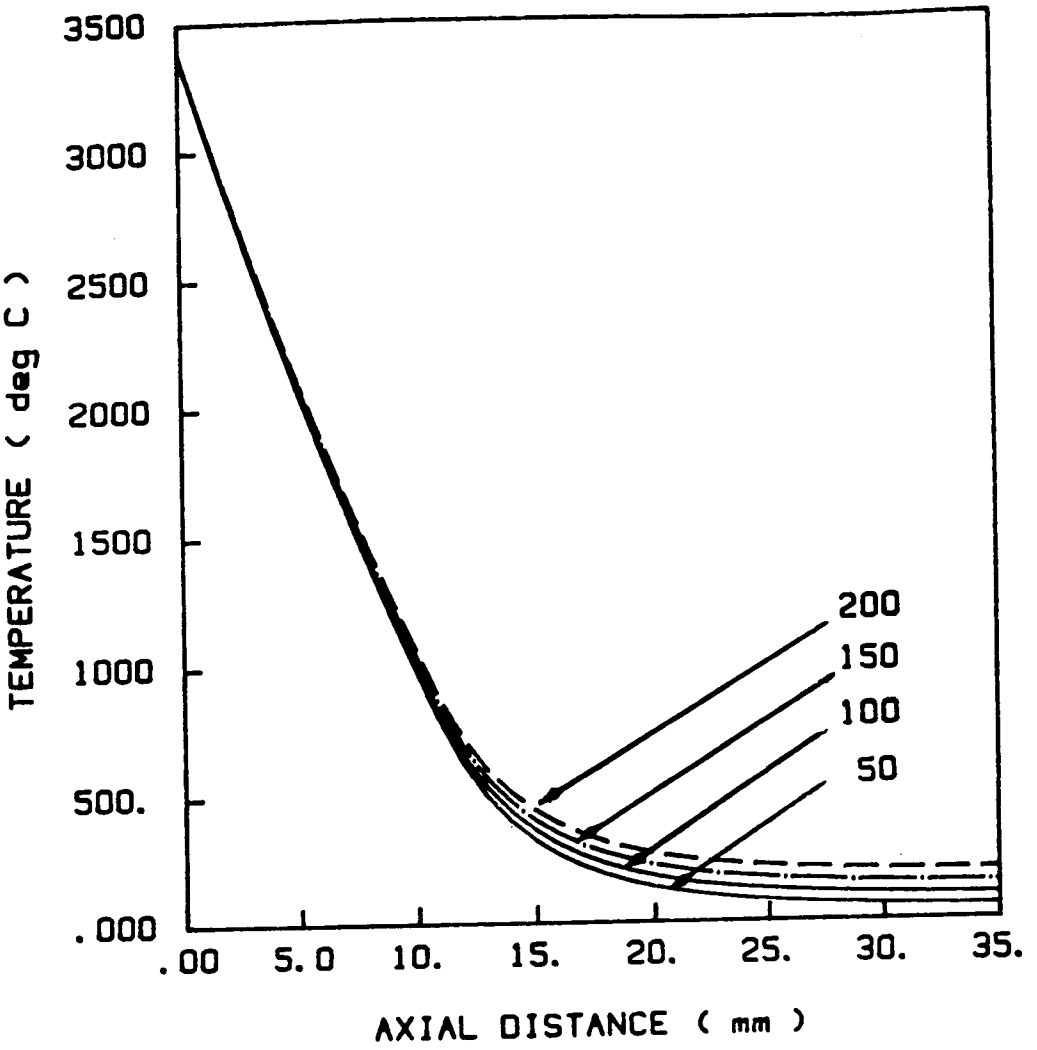

Figure 8. Centerline temperature profiles for different quench block temperatures.

location at 0 mm.

Several isotherms for the model were included in the contour plots shown in Figure 9. These temperature contours range from the quench block temperature to 3387 C and are plotted at their respective positions in the modeled portion of the sample. The calculations indicate that a relatively small, and extremely localized melt zone exists. In the first millimeter along the axial direction form the melt interface the temperature drops 187°C from the melting point of tungsten at 3387°C to 3200°C.

Figures 9 a, b, c, and d show contour plots obtained for the Arc Furnace with isothermal boundaries of 50, 100, 150, and 200°C, respectively. In all four figures the 500°C isotherm penetrates well into the holder region. This temperature is approaching the melting point for aluminum holders. Even at temperatures as low 10 and 38°C (see Figures 10 a and b) this penetration is still apparent. We are in the process of modeling aluminum holders and it will be interesting to see if a region near the melting point is predicted.

In all six figures one consistent trend can be seen. The isotherms in the sample from the center of the sample (0 mm in Figures 9 and 10) to about 10 mm are relatively constant no matter what cooling fluid temperature is used. This trend was also apparent in Figure 8. As previously discussed, the sample processing region are not greatly influenced by the quench block temperatures studied. Therefore, several different scenarios for cooling the Arc Furnace are possible, including forced air, water, or change of phase cooling approaches. As an example, one might chose to design a quench block and holder combination which would use the conversion of water to steam to remove heat and provide a constant reference temperature at the cooling block. Calculations of the volumetric flow rates for water and forced air cooling still need to be made and are topics of further study.

Radial profiles for these numerical calculations are shown in Figure 11 a, b, c, and d for the 50, 100, 150, and 200°C, respectively, and Figure 12 for the 10 and 38°C simulations. Again, these figures remain virtually unchanged in the region discussed above. In these figures, the zero line represents the centerline temperature, with the solid line representing the tungsten surface. The dashed line is difference between the centerline profile and the profile at a

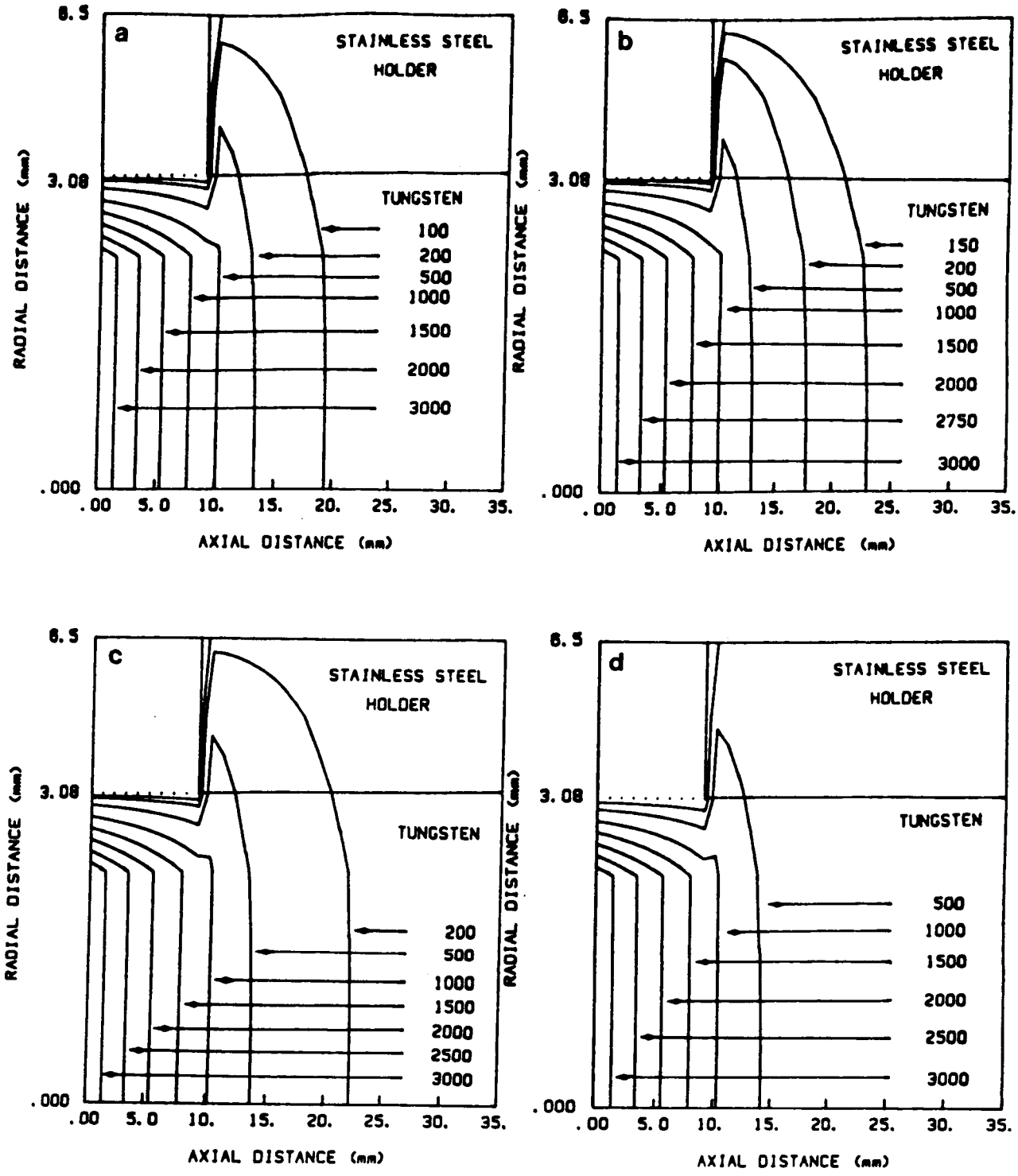

Figure 9. Contour plots obtained for the Arc Furnace with a tungsten sample and stainless steel holder. Boundary conditions on the external surface of the holder were controlled at a) 50°C, b) 100°C, c) 150°C, and d) 200°C.

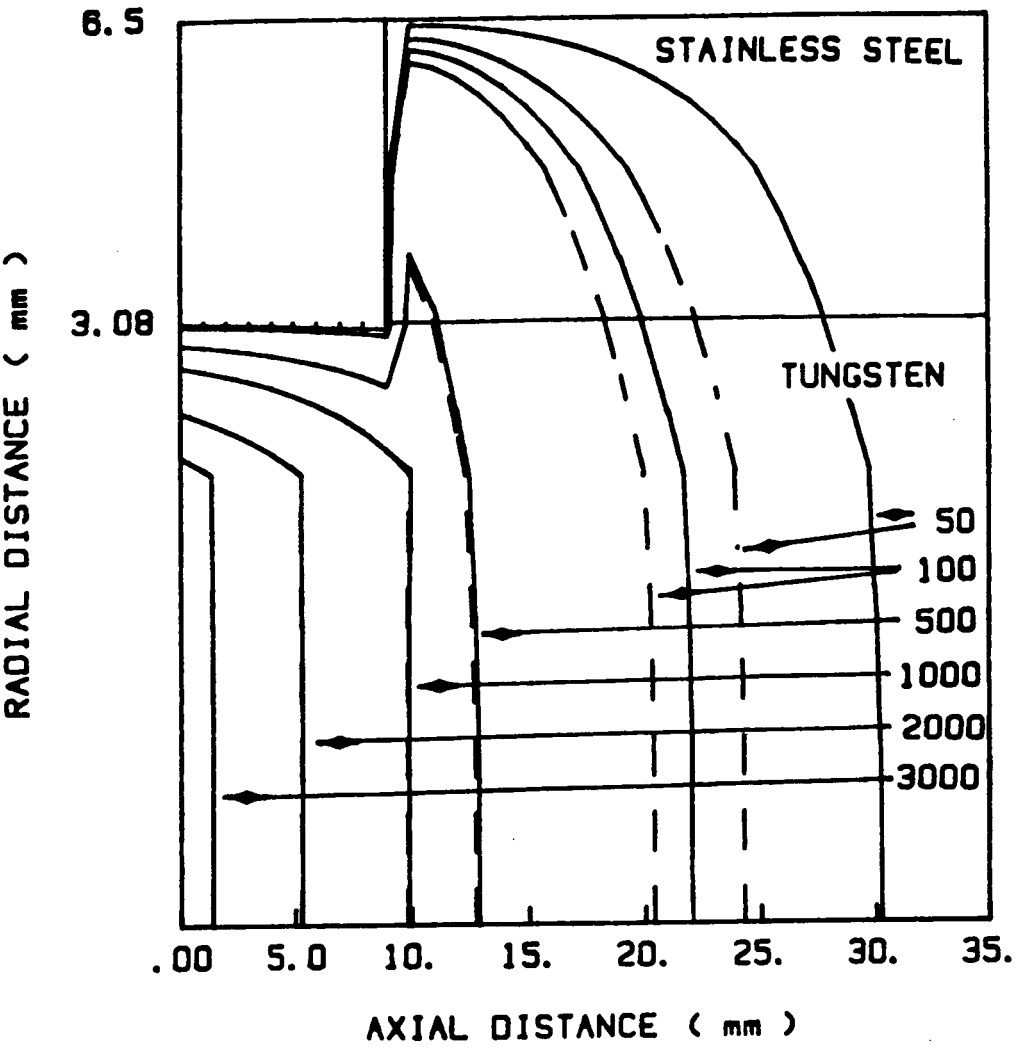

Figure 10. Contour plots obtained for the Arc Furnace with a tungsten sample and stainless steel holder. Boundary conditions on the external surface of the holder were controlled at 10°C (dashed line) and 38°C (solid line).

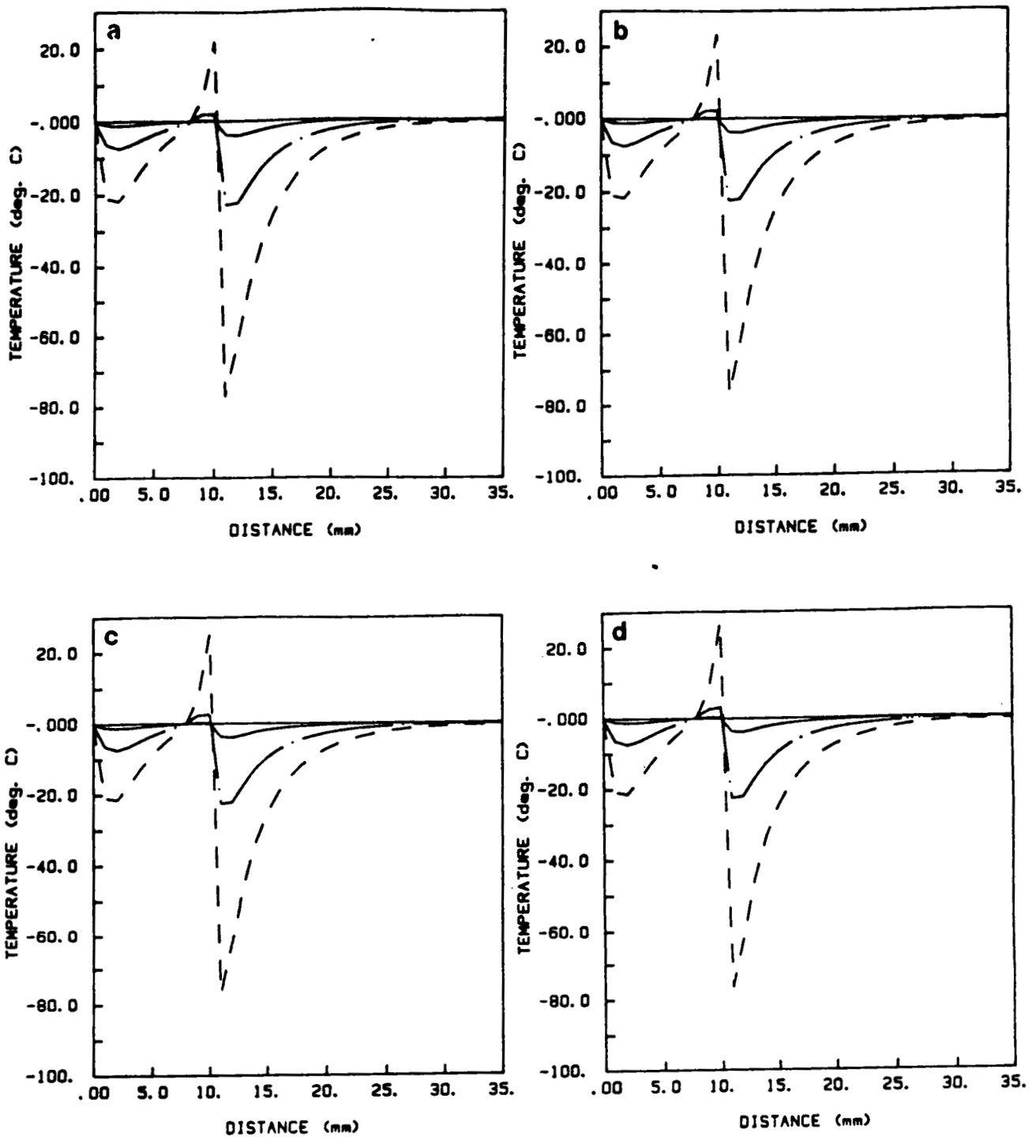

Figure 11. Radial temperature distributions relative to the centerline temperature for the Arc Furnace with a tungsten sample and stainless steel holder. Boundary conditions on the external surface of the holder were controlled at a) 50°C, b) 100°C, c) 150°C, and d) 200°C.

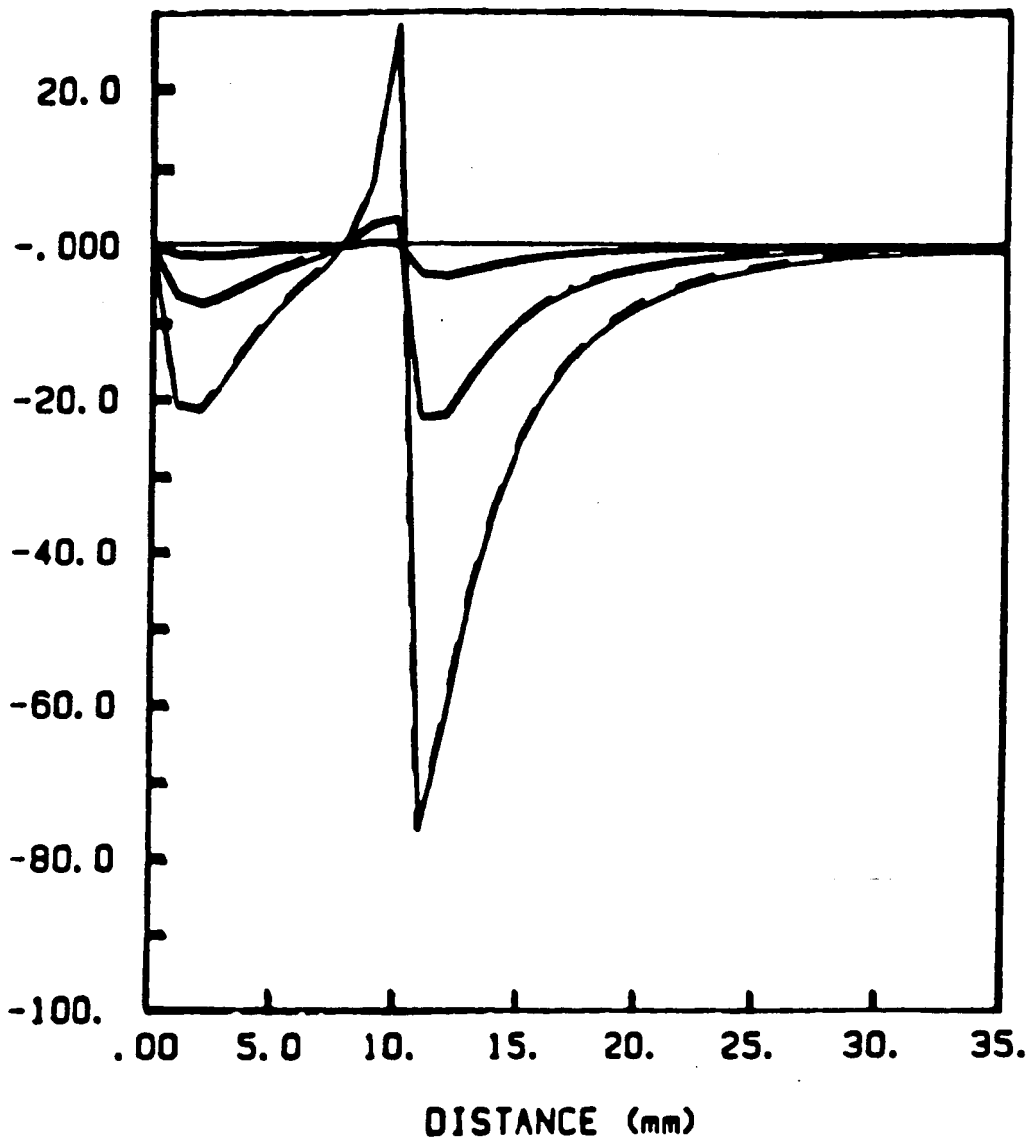

Figure 12. Radial temperature distributions relative to the centerline temperature for the Arc Furnace with a tungsten sample and stainless steel holder. Boundary conditions on the external surface of the holder were controlled at 10°C (dashed line) and 38°C (solid line).

radial distance of 2mm, while the additional line is for the difference in the radial profile at 1mm relative to the centerline. The largest deviation in the radial profile occurs on either side of the sample entrance into the stainless steel holder and quench region.

3.0 FUTURE WORK

We are actively working to resolve the instabilities discussed under objective 3. Additional studies on the quench block's materials of construction are planned. Brass and alloy of aluminum may receive additional consideration as we zero in on design options. A major goal is the integration of the zirconia furnace with a computer and the optical pyrometer to permit direct measurement and control of the zirconia furnace. Standards must be developed to permit accurate calibration of the furnace to permit scientific investigation under tightly controlled conditions. To this end, crucibles containing known materials will be slowly solidified while monitoring the wall temperature of the zirconia furnace with the optical pyrometer. With this approach we will be able to develop a calibration curve for the furnace. The extent to which the zirconia furnace can be controlled will depend largely on the accuracy and stability of this calibration as a function of time. Finally preliminary work will begin on the Arc Furnace in an effort to understand its performance and data acquisition and control routines.

4.0 REFERENCES

J. P. Holman, Heat Transfer, McGraw Hill, New York, N.Y., (1981).

R. M. Poorman, "Rapid Melt/Quench Furnace Using Commercially Available Hardware," NASA Technical Memorandum, George C. Marshall Space Flight Center, Marshall Space Flight Center, AL, March 1986.